

LARGE-APERTURE BIMORPH ADAPTIVE MIRROR: COMPUTER-AIDED DESIGN

A.V. Ikramov, I.M. Roshchupkin, and A.G. Safronov

Scientific-Production Company "Kompozit", Kaliningrad

Received February 19, 1993

The design of a large-aperture adaptive mirror which can be used as a main mirror of astronomical telescope to compensate for large-scale low-frequency phase distortions of the wavefront is proposed. The adaptive mirror is described, and methods and results of numerical investigation of response functions of controlling electrodes, thermal deformations of a reflecting surface, and frequency properties of the mirror are presented.

Existing adaptive telescopes¹⁻⁴ and projects of the future ones,⁵⁻⁹ as a rule, are based on the adaptive mirror with discrete actuators compensating for the phase distortions of the wavefront. Such an adaptive mirror may be both the main mirror of a telescope and the special one, inserted into its optical scheme. In spite of a variety of the controlling actuator design, the principle of controlling the optical surface of a mirror remains unchanged: the controlling forces are exerted by the actuators at fixed points.

Today there is only one project of the adaptive telescope in which the bimorph adaptive mirror is used for control of the wavefront.^{9,10} The project is based on an infrared telescope with a main mirror 3.6 m in diameter and is carried out by the Hawaii University. The phase distortions of the wavefront are compensated by a deformable bimorph mirror 30 mm in diameter with 13 zones of control (electrodes).⁶ Such a choice of the adaptive mirror is explained by the use of a sensor of curvature as a wavefront analyzer that matches well the bimorph mirror.¹¹

In this paper we propose a design of a large-aperture bimorph mirror for an astronomical telescope. Previously we developed and fabricated bimorph adaptive mirrors for technological lasers,^{12,13} so this material is based on the experience of our previous research. An analysis of the large-aperture mirror is based on a 3.3-m model mirror developed by the Scientific-Production Company "Optika" (Moscow). For this mirror we developed a 60-channel digital system of controlling the shape of a reflecting surface.

For vivid presentation of further analysis we briefly describe the characteristics of this mirror and the results of the numerical investigations of its response functions. The overall dimensions of the mirror were the following: central aperture was 500 mm in diameter, thickness was 78 mm, and radius of curvature of a reflecting surface was 30 252 mm. It was fabricated from CO-115 M glassceramic. The mirror operation assumes two systems of unloading - horizontal and vertical ones. The horizontal system of unloading consisted of 120 pneumatic face supports of different heights that were connected with a truss-type stiff supporting frame.

The main functional part of a pneumatic support was a pneumatic support base kept under excess pressure that was the same for all supports connected with each other by the system of flexible tubing. The stiffness of the pneumatic supports was 200-300 g/mm with force of gravity and much less in other directions. The optimum arrangement of the pneumatic supports (in 5 circles located equidistantly in each circle) provided the required quality of the working

surface of the mirror under operating conditions in the field of force of gravity. It should be also noted that the use of the pneumatic supports enabled us to avoid the effect of parasitic deformations of a supporting frame on the quality of the optical surface of the mirror. In vertical position of the supporting frame the mirror was retained by 60 supports of the vertical unloading system embodying the principle of lever, that were mounted in bushings of a frame body. One end of a supporting cantilever beam, which was hinged in the bushing of the frame, was clamped at the central part of the mirror surface and its another end was connected with a pneumatic support base placed in the bushing of the frame body. In such a pneumatic system of unloading the behavior of the mirror follows that of a mirror floating in liquid.

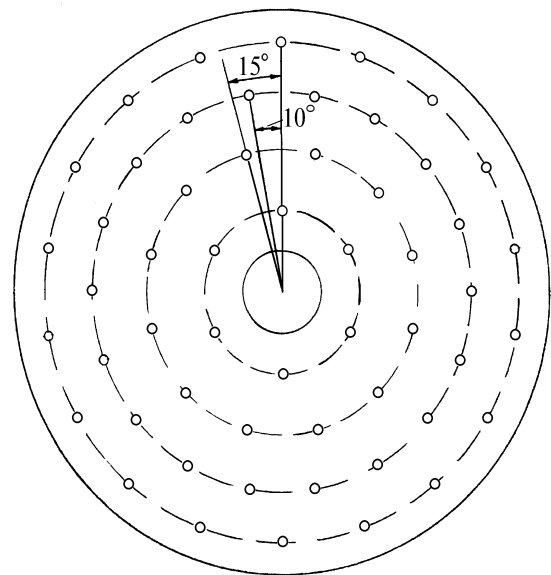


FIG. 1. Scheme of arrangement of actuators of the spherical adaptive mirror 3.3 m in diameter, $R_1 = 250$, $R_2 = 480$, $R_3 = 830$, $R_4 = 1145$, $R_5 = 1460$, and $R_6 = 1650$ mm.

The control system of the mirror contained 54 electromechanical final control elements (Fig. 1), an electronic unit for 60 control channels, and a control computer. The control actuators were based on the SDR-

711 stepping motor (for more details, see Ref. 14). The electronic unit converted the directives of the computer to four-phase surge voltage supplying the final control elements. We used IBM PC AT 286/287 as the control computer.

Figure 2 shows the typical function of response of the large-aperture adaptive mirror to displace a rod of the controlling actuator by 10 mm for the actuator arranged in a circle of 480 mm radius (disregarding tilts and constant displacement).

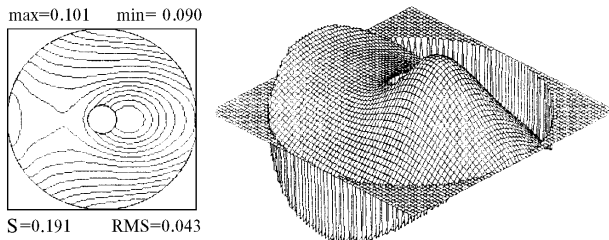


FIG. 2. Typical response function of the spherical adaptive mirror for the actuator arranged a circle of 480 mm radius to displace the rod by 10 mm (disregarding tilts and constant displacement). The span (S), root-mean-square deviation (RMS), and the maximum and minimum values are given in micrometers.

Let us use this mirror to fabricate the bimorph large-aperture adaptive mirror, all the characteristics of the mirror plate and the unloading system remaining unchanged.

Let a piezoceramic layer consisting of hexagonal elements of equal thicknesses be formed on the rear of the mirror plate (see Fig. 3), with the thickness of this piezoceramic layer being 1 mm. The material properties correspond to TTS-19 ceramic (see Table I). For ease of calculations the piezoceramic layer is considered to be a plate 3.3 m in diameter with central aperture 500 mm in diameter. This assumption is quite acceptable, because all elements of the piezoceramic layer are rigidly connected with each other and with the mirror plate and their envelope has near-circular shape.

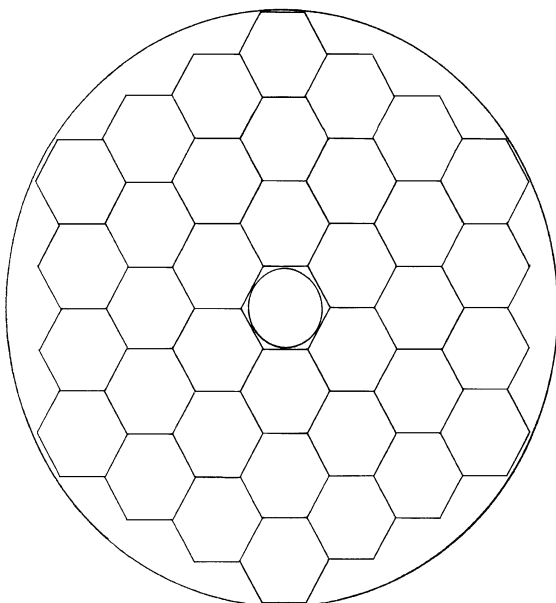


FIG. 3. Shaping of the piezoceramic mosaic controlling layer on the rear of the 3.3-m adaptive mirror.
TABLE I. Properties of TTS-19 piezoceramic.

Parameter, unit	Symbol	TTS-19
Curie point, K ($^{\circ}\text{C}$), no less than	T_C	563 (290)
Recommended operating temperature, K ($^{\circ}\text{C}$)	ΔT	213(-60)–473 (200)
Relative permittivity	$\epsilon_{33}^T/\epsilon_0$	1620–1980
	$\epsilon_{11}^T/\epsilon_0$	1400–1700
Piezoelectric modulus, 10^{-12} Coul/N	$ d_{13} $	150–200
	d_{33}	310–460
Poisson's ratio	σ_P	0.35–0.41
Density, 10^{-3} kg/m ³	ρ	7.3–7.8
Coefficient of thermal expansion, 10^{-6} K ⁻¹	α	4–5

We have chosen the method of finite elements (MFE) for numerical simulation of the design of the adaptive bimorph mirrors. This method is based on the approximation of a continuous medium with the infinite number of degrees of freedom by a collection of simple elements with the finite number of degrees of freedom which are connected with each other at nodes. Such a choice is due to the following advantages of the MFE: wide range of applicability, invariance under geometry of design and mechanical properties of materials, and the ease to account for interaction with the environment (mechanical and thermal loads, boundary conditions, and so on). Mathematically, the MFE is the generalized Rayleigh–Ritz–Galerkin method in which the functional of potential energy Φ is minimized by way of finding of the combination of the trial functions ϕ_i

$$\Phi = \sum_{i=1}^N a_i \phi_i, \quad (1)$$

where a_i are the coefficients determined by solving the system of N algebraic equations.

In the modification of the MFE method referred to as the method of displacements resolvent equations are derived by minimizing the total potential energy of the system expressed in terms of a field of displacements. These equations have a simple physical meaning — they describe the equilibrium of the nodes of the system whereas the required unknowns are the components of the nodal displacements corresponding to the weighting coefficients in the Ritz method.

We used the computer-aided design system DIANA of discrete analysis that enables one to design a wide variety of systems including two- and three-dimensional systems of rods, linear and volume strains, plates, shells, and so on. In solving these problems, the global matrices of stiffness, mass, thermal conductivity, and so on are optimized. This enables one not to care for the optimum (from the execution time standpoint) numbering of nodes of the design scheme. Each node of the system is assumed to have the degrees of freedom (generalized displacements) of the types that possess the nodal points of final control elements connected with this node. Displacements of various kinematic types, for example, the components of translational motion in the directions of axes of the global coordinate system of the design or rotations about these axes can be considered as the generalized displacements.

Numerical investigations of the response functions of the main large-aperture bimorph adaptive mirror of the telescope were performed for the finite-element model, used before to find the response functions of a mirror with discrete actuators and subject to some modifications concerning the geometry of the piezoceramic plates.

To find the response functions (i. e., deformations of the reflecting mirror surface when the controlling voltage is applied to a given electrode) of the adaptive bimorph mirror fabricated from glassceramic, we have chosen the finite–element model of 372 nodes (Fig. 4). The mirror from glassceramic was modeled by 288 elements of the SBSE4 thick isotropic quadrangular plate being eccentric from the nodal surface. The piezoceramic plates were also modeled by 288 elements of the SBSE4 thick isotropic plate. The nodal surface of the finite–element model was located on the rear of the mirror.

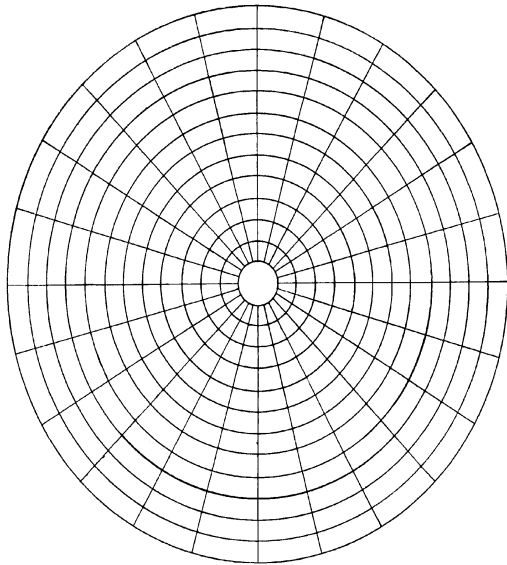


FIG. 4. Finite–element model of the large–aperture bimorph adaptive mirror. $R_1 = 250$, $R_2 = 415.8$, $R_3 = 480$, $R_4 = 600.6$, $R_5 = 721.2$, $R_6 = 830$, $R_7 = 990.5$, $R_8 = 1145$, $R_9 = 1255.6$, $R_{10} = 1370$, $R_{11} = 1460$, $R_{12} = 1550.9$, and $R_{13} = 1650$ mm.

Each node had six degrees of freedom: U , V , and W were the displacements in the X , Y and Z directions and Φ_X , Φ_Y , and Φ_Z were rotations about the X , Y , and Z axes. The elements did not stiffen with rotations about the normal to the surface. The stiffness matrix of the elements was obtained by integrating the membrane stiffness matrix over the thickness of the element. The contribution of the lateral shear stiffness was taken into account by the use of additional stiffness matrix of the isoparametric element possessing only the lateral shear stiffness. To suppress the effect of spurious shear on the isoparametric element, we decreased the accuracy of numerical integration.

We modeled the pneumatic supports of the clamping system of the mirror by the TR6M element having two nodes of the same geometry being springly connected. Each node of the element had three translational motions U , V , and W in the X , Y and Z directions and three rotations Φ_X , Φ_Y , and Φ_Z about X , Y , and Z axes of the global coordinate system. The voltage applied to the controlling electrodes was modeled by prescribed initial deformations at the nodes of the elements that described the geometry of zones corresponding to the position of electrodes. The initial deformations and the applied electric voltage are related in the following way:

$$\varepsilon_{ZZ} = d_{33} E, \quad (2)$$

$$\varepsilon_{XX} = \varepsilon_{YY} = d_{13} E, \quad (3)$$

$$E = U/h, \quad (4)$$

where ε_{XX} , ε_{YY} , and ε_{ZZ} are the components of the tensor of initial deformations; d_{13} and d_{33} are piezoelectric moduli of piezoceramic plates, E is the electric field strength inside the piezoceramic plates; U is the applied electric voltage, and h is the thickness of the plate.

We optimized the configuration of electrodes of the piezoceramic plate to minimize the rms deviation of the residual error of reproduction of the following aberrations: defocusing, astigmatism, coma, trefoil, and spherical aberration, represented in terms of Zernike polynomials, by the reflecting mirror surface. Taking into account the properties of the above–enumerated aberrations, we represented individual electrodes as rings and sectors that combine individual finite elements describing the geometry of piezoceramic plate. To decrease the error in compensation for axisymmetrical aberrations, we varied the number of the ring controlling electrodes that consisted of several finite elements with equal prescribed initial deformations. Accordingly, we took the set of the finite elements, describing these electrodes, in the form of sectors for minimization of the error in compensation for astigmatism, coma, and trefoil. In this case we also varied the number of the finite elements of the controlling electrode.

The frequency characteristics of the large–aperture bimorph mirror were analyzed for the model used to determine the response functions. The main problem was to find the first lower frequencies and the corresponding modes of free oscillations of the design, described by the equation

$$M \ddot{X} + K X = 0, \quad (5)$$

where M is the matrix of mass, K is the matrix of stiffness of the design, and X is the matrix of the oscillation modes.

This problem reduced to the problem of finding the first greatest eigenvalues and corresponding eigenvectors of the system of equations

$$M X = K X L, \quad (6)$$

where L is the diagonal matrix of eigenvalues, $L_{ii} = 1/W_{ii}^2$, and W_{ii} are the angular frequencies of free oscillations. We determined the modes and frequencies of free oscillations by the iteration method in subspace. The effect of the ambient temperature variations on the deformed state of the large–aperture bimorph adaptive mirror was investigated for the finite–element model discussed above (see Fig. 4).

As a result of these calculations, we have found that the minimum of the rms deviation of the residual error in reproduction of the above–indicated aberrations is achieved when the controlling electrodes are modeled by the individual finite elements, i. e., when the segmentation of the controlling electrodes corresponds to Fig. 4. Figure 5 shows the typical response function of the large–aperture bimorph adaptive mirror for a controlling voltage of 300 V in two variants — as isometric projection and contours. The figure shows the span (S), rms deviation (RMS), and maximum and minimum values of the response function measured along the normal to the reflecting mirror surface. All values are given in micrometers. The frequency of the first resonance of the adaptive mirror is 1 Hz.

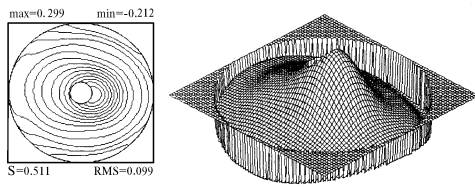


FIG. 5. The typical response function of the large-aperture bimorph adaptive mirror for a controlling voltage of 300 V of the electrode of 415.8 mm outside radius. The span (S), rms deviation (RMS), and maximum and minimum values are given in micrometers.

Numerical investigations of the effect of the ambient temperature on the deformed state of the mirror have shown, in particular, that as temperature changes by 1°C , the span of the displacement of the reflecting surface reaches $3.96\ \mu\text{m}$. In this case the characteristic warming-up time is a few minutes.

The obtained results indicate the following. First, the response functions of the controlling electrodes (see Fig. 5) are essentially nonlocalized, as could be expected, and so the mirror will compensate well for the large-scale phase distortions of the wavefront whose spatial frequency is of the order of $1/2D$ (where D is the mirror diameter). Second, the fundamental resonance frequency of the mirror (1 Hz) is low enough, what is explained by the unloading system resulting in the "floating" mirror that is effective only for correction of the slowly varying phase distortions of the wavefront.

The results of calculations of the thermal deformations of the mirror as the temperature changes by 1°C show that although the mirror deformation is about 4 mm, it can easily be corrected because:

(1) thermal deformations of the mirror are shaped like defocusing,

(2) range of correction of the axisymmetrical aberrations of the wavefront is very wide, for defocusing it is about $70\ \mu\text{m}$, and

(3) periods of variation of these aberrations are large enough.

So, 10% of the controlling voltage range is enough to compensate for the thermal deformations of this large-aperture bimorph adaptive mirror.

In conclusion it should be noted that we used a maximum model controlling voltage of $\pm 300\ \text{V}$ though it is not a limit for the examined 1-mm thick piezoceramic. The capabilities of control of the mirror deformations will increase for larger controlling voltage. In addition, the piezoelectric controlling mosaic layer may be made of multi-layer composition. As a result, the controlling voltage may be several times lower, and in this case the deformation amplitude will not decrease. In the last case the electrodes must be disconnected to apply voltage to them.

REFERENCES

1. A. Buffington, F.S. Crawford, R.A. Muller, et al., *JOSA* **67**, No. 3, 298–303 (1977).
2. Yu.V. Baranov, S.B. Novikov, and A.A. Ovchinnikov, in: *Atmospheric Instability and Adaptive Telescope* (Gidrometeoizdat, Leningrad, 1988), pp. 25–27.
3. N.V. Steshenko and V.V. Sychev, in: *Atmospheric Instability and Adaptive Telescope* (Gidrometeoizdat, Leningrad, 1988), pp. 5–10.
4. *Netherlands Meeting Highlights Adaptive Optics*, *Las. Foc. W. No. 6*, 51–52 (1990).
5. M.A. Ealey, *Proc. SPIE* **1543**, 2–34 (1991).
6. P. Jagourel and J.P. Gaffard, *Proc. SPIE* **1543**, 76–87 (1991).
7. R.B. Dunn, G.W. Streander, W. Hull, et al., *Proc. SPIE* **1543**, 88–100 (1991).
8. R.L. Plante, *Proc. SPIE* **1543**, 146–160 (1991).
9. J.W. Hardy, *Proc. SPIE* **1542**, 2–17 (1991).
10. F. Roddier, *OE Rep.*, No. 103, 9–11 (1992).
11. F. Roddier, *Appl. Opt.* **27**, No. 7, 1223–1225 (1988).
12. A.V. Ikramov, A.V. Kudryashov, S.B. Romanov, et al., Author's Certificate No. 1808159 (1992).
13. A.V. Ikramov, S.B. Romanov, I.M. Roshchupkin, et al., *Kvant. Elektron.* **19**, No. 2, 180–183 (1992).
14. A.V. Ikramov, S.B. Romanov, I.M. Roshchupkin, et al., *Opt. Mekh. Promst.*, No. 5, 60–63 (1992).
15. A.V. Ikramov, I.M. Roshchupkin, and A.G. Safronov, *Atmos. Oceanic Opt.* **6**, No. 9, 636–640 (1993).